Narrow-band imaging with magnification in Barrett's esophagus: validation of a simplified grading system of mucosal morphology patterns against histology

Authors

R. Singh[1], G. K. Anagnostopoulos[1], K. Yao[1], H. Karageorgiou[1], P. J. Fortun[1], A. Shonde[1], K. Garsed[1], P. V. Kaye[2], C. J. Hawkey[1], K. Ragunath[1]

Institutions

[1] Wolfson Digestive Diseases Centre, Queen's Medical Centre, Nottingham, UK
[2] Department of Histopathology, Queen's Medical Centre, Nottingham, UK

submitted
20 November 2007
accepted after revision
4 February 2008

Bibliography
DOI 10.1055/s-2007-995741
Published ahead of print
Endoscopy

ISSN 0013-726X

Corresponding author
K. Ragunath, MD, FRCP
Wolfson Digestive
Diseases Centre
Queen's Medical Centre
Campus
Nottingham University
Hospitals NHS Trust
Nottingham
NG7 2UH
UK
Fax: +44-115-9422232
K.Ragunath@nottingham.ac.uk

Background and study aims: Validation of a simplified classification of mucosal morphology in prediction of histology in Barrett's esophagus using narrow-band imaging with magnification (NBI-Z) and assessing its reproducibility by endoscopists experienced in the use of NBI (NBI-experts) and by endoscopists who were new to NBI (non-NBI-experts).

Patients and methods: In a prospective cohort study of 109 patients with Barrett's esophagus at a single tertiary referral center, mucosal patterns visualized in Barrett's esophagus on NBI-Z were classified into four easily distinguishable types: A, round pits with regular microvasculature; B, villous/ridge pits with regular microvasculature; C, absent pits with regular microvasculature; D, distorted pits with irregular microvasculature. The NBI-Z grading was compared with the final histopathological diagnosis, and positive (PPV) and negative predictive values (NPV) were calculated. The reproducibility of the grading was then assessed by NBI-expert and non-NBI-expert endoscopists, and interobserver and intraobserver agreement were calculated using κ statistics.

Results: *Per-biopsy analysis:* In 903 out of 1021 distinct areas (87.9%) the NBI-Z grading corresponded to the histological diagnosis. *Per-patient analysis:* The PPV and NPV for type A pattern (columnar mucosa without intestinal metaplasia) were 100% and 97% respectively; for types B and C (intestinal metaplasia) they were 88% and 91% respectively, and for type D (high-grade dysplasia) 81% and 99% respectively. *Inter- and intraobserver agreement:* The mean κ values in assessing the various patterns were 0.71 and 0.87 in the non-expert group; 0.78 and 0.91 in the expert group.

Conclusions: This study has validated a simplified classification of the various morphologic patterns visualized in Barrett's esophagus and confirmed its reproducibility when used by NBI-expert and non-NBI-expert endoscopists.

Introduction

The incidence of esophageal adenocarcinoma has quadrupled over the last four decades [1,2]. At less than 14% [3], the 5-year survival for this cancer is dismal. Barrett's esophagus is the only identifiable premalignant condition responsible for this increase, and it is known that outcomes for esophageal adenocarcinoma are better in patients with Barrett's esophagus who are on a surveillance protocol [4]. The guidelines practiced by most societies suggest that surveillance for these patients should be random quadrantic biopsies, every 2 cm of the Barrett's segment [5,6]. However, this has been described as a "hit and miss" approach as areas of high-grade dysplasia or microscopic carcinoma in Barrett's esophagus are often small [7] and can remain undetected even by the most rigorous biopsy protocols. In recent years, with the advent of a plethora of new technologies which allow more specific targeted biopsies, the identification of dysplasia and cancer in patients with Barrett's esophagus has improved [8]. Although the increased yield is impressive, there have been some concerns regarding uniformity in the methods used. The technical skill required to perform these procedures can sometimes be daunting as well.

Recently, a novel promising technology, narrow-band imaging (NBI), has come to the forefront of attention [9]. It provides the endoscopist with a quick and simple way to visualize the mucosa. At the switch of a button, images can be obtained in real time almost instantaneously. The addition of the magnification/zoom component has further allowed visualization of very minute mucosal details and hence prediction of histology in real time. Preliminary descriptive studies done with NBI and magnification by our group [10] and both the Amsterdam [11] and Kansas groups

[12] have shown a high correlation between NBI findings and histology.

The aim of the present study was to validate a simplified mucosal morphology classification in detecting the following: columnar mucosa without intestinal metaplasia, intestinal metaplasia, low-grade dysplasia, and high-grade dysplasia in Barrett's esophagus in a large cohort of patients and then to test its reproducibility both by endoscopists who are expert in NBI and by those not expert in it.

Methods

Patients

The study was approved by our institutional research and ethics committee. Patients known to have Barrett's esophagus and undergoing surveillance endoscopy or referred from other centers for workup of recently diagnosed dysplasia between 15 May 2006 and 14 May 2007 were invited to participate in the study. Barrett's esophagus was defined in accordance with the new British Society of Gastroenterology guidelines as "an endoscopically apparent area above the oesophago-gastric junction that is suggestive of Barrett's and is supported by the finding of columnar lined oesophagus on histology" [13]. All patients gave written informed consent. Patients were excluded if they had conditions that could preclude adequate sampling of the esophagus (coagulation disorders, anticoagulant therapy, esophageal varices), if they exhibited any endoscopic evidence of erosive esophagitis, or if they had obvious esophageal cancer.

Classification

A consensus meeting was first arranged between the four expert endoscopists (R. S., G. A., K. Y., and K. R.) who have had experience in magnification endoscopy. It was decided that the grading of the various pit patterns and vasculature be simplified. It appeared that previous classifications [10–12] were tedious and difficult to apply in routine practice. Based on our observational study [10], we realized that four distinct pit and vascular patterns could be visualized in the Barrett's segment when NBI with magnification/zoom (NBI-Z) was used. We therefore classified the mucosal morphology into these four easily distinguishable types:

Type A: Round pits with regular microvasculature (**Fig. 1**)

Type B: Villous/ridge pits with regular microvasculature (**Fig. 2**)

Type C: Absent pits with regular microvasculature (**Fig. 3**)

Type D: Distorted pits with irregular microvasculature (**Fig. 4**)

In the description of the morphology of the pit pattern, round or oval-shaped pits visualized would be in keeping with type A. The type B morphology demonstrated villous, ridged, or linear pits, while in the C type the pit morphology is not visualized at all. The D type exhibited total distortion of the regularity of the pit structure. In the description of the vascular network, the type D pattern differed from the preceding three patterns on the basis of the abnormal caliber as well as the tortuosity of the microvasculature that was observed.

Endoscopy equipment

All examinations were performed with the prototype NBI system (Olympus Corp., Tokyo, Japan). This system is equipped with a red, green, and blue (RGB) sequential-illumination xenon light source (XCLV-260HP), a high-resolution zoom gastroscope (GIF-

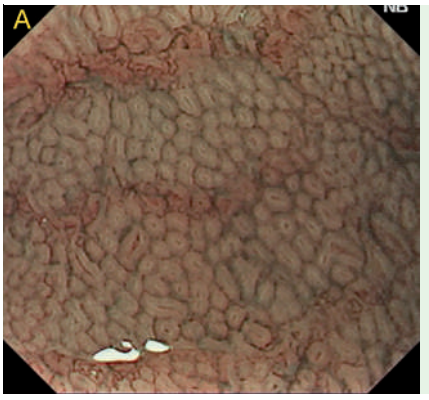

Fig. 1 Type A: round pits with regular microvasculature.

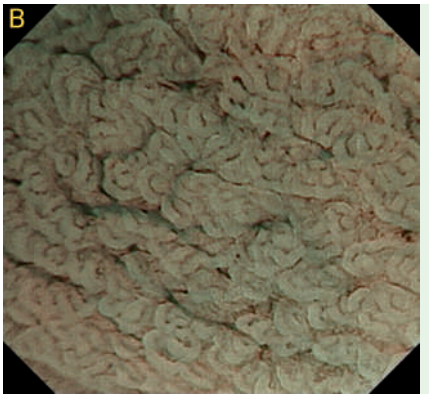

Fig. 2 Type B: villous/ridge pits with regular microvasculature.

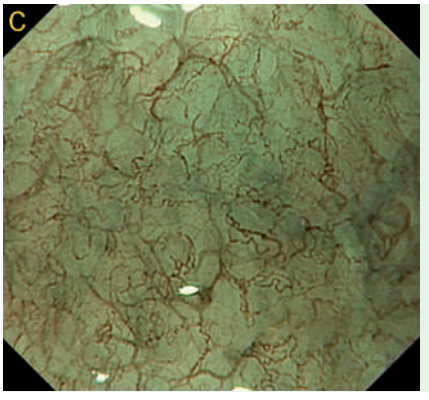

Fig. 3 Type C: absent pits with regular microvasculature.

Fig. 4 Type D: distorted pits with irregular microvasculature.

Q240Z), a video processor (XCV-260HP3P), and a high-definition television monitor (Olympus OEV181H). The light source contains one rotating RGB filter and one NBI filter. The NBI filter is placed between the RGB filter and the light source. It splits white light into two specific lights with narrowed bandwidths; blue (400 – 430 nm) and green (530 – 550 nm), while the contribution of the red light, which has a longer bandwidth and hence deeper penetration, is reduced. This allows the blue and green lights, which have more superficial penetration, to penetrate the superficial mucosal architecture, leading to enhancement of both the pit patterns and the vasculature [14]. The insertion of the NBI filter between the RGB filter and the xenon lamp is achieved by activating a switch on the scope. The endoscopist can then alternate between white-light endoscopy (WLE) and NBI easily at any time. The NBI-Z function is activated by depression of a lever on the gastroscope which adjusts the zoom lens at the distal tip of the scope. By altering the focal distance of the lens, a maximal magnification of up to × 115 can be achieved. Prior to endoscopy, a black cap (MB-046 Olympus, Japan) was fitted and adjusted to a 2-mm distance from the tip of the endoscope. This was performed by visualizing a thin rim of the cap on endoscopic views once it had been snugly fitted to the tip, which made it possible for the endoscopist to fix the mucosa to the endoscope before applying the zoom mode. Optimal focus was thus easily obtainable using this technique.

Endoscopic examination

With informed consent, all patients were offered either conscious sedation with intravenous midazolam or local pharyngeal anesthesia with xylocaine spray. All endoscopies were performed by the four expert endoscopists and recorded using a digital video cassette recorder (Sony Mini DV GV-D1000E PAL; Sony Corp., Tokyo, Japan). With such high magnification, it is imperative to visualize the mucosa clearly, hence patients were given a mucolytic agent, *N*-acetylcysteine, and a defoaming agent, simethicone, mixed with water (50 ml) to drink prior to the procedure. Following intubation of the esophagus, an additional 10–20 ml of this mixture was flushed to rid the surface of any adherent mucus. To minimize movement artifacts, and if felt necessary, the sedation was titrated up at the discretion of the endoscopist. If the esophagus exhibited excessive peristaltic activity which interfered with the examination, an antispasmodic agent, hyoscine-*N*-butylbromide (Buscopan, 10 – 20 mg), was administered intravenously. The esophagus was first examined with WLE and NBI in the overview mode (without activation of the zoom lens) and the endoscopist recorded the length of Barrett's segment according to the Prague criteria [15] and any macroscopically evident lesions. Only macroscopically inconspicuous and flat areas or areas adjacent to macroscopically visible lesions on WLE in the Barrett's segment were assessed by the NBI-Z mode.

The examination with the NBI-Z mode was done by gently withdrawing the endoscope from the gastroesophageal junction. After visualization of each quadrant of the Barrett's segment at a given distance with the NBI-Z mode, a digital still image was recorded. This was followed by taking biopsies of the areas corresponding to the magnified and imaged views. We ensured that the imaged view was the area biopsied by applying light suction pressure to the mucosa, thus enabling the cap to fix the imaged area. After taking one targeted biopsy of the area, we then zoomed in on another quadrant and repeated the procedure (digital still image followed by targeted biopsy). This was done every 2 cm in each quadrant of Barrett's esophagus, starting from the gastroesophageal junction.

The endoscopist did not classify the images obtained in real time. All images were stored as JPEG files (200 – 300 kb, 1280 × 1024 pixel array and 32-bit color). We were especially careful in visualization of the mucosa, and if blood from earlier biopsies obscured the views, adequate flushing with water was done until a clear visual field was obtained. We also alternated freely between the zoom and unzoom modes to ensure that we were consistently aware of the previous biopsy sites and the actual position of the scope in the Barrett's segment. All biopsies were taken using standard biopsy forceps (FB230K; Olympus) and placed in separate labeled pots filled with 10 % buffered formalin. As we dealt with a large number of samples during each procedure, we ensured that each pot was clearly labelled and linked to the corresponding NBI image.

Postprocedural assessment

All images were subsequently transferred using movie-making software (U Lead Video Studio 7SE DVD; U Lead Systems Inc., California, USA) to another program (Powerpoint; Microsoft, Redmond, Washington, USA). Blinded grading of each image was then performed (RS) and transferred to a computerized database. Care was taken in grading these images. Concerns about visualizing more than one pattern in each image (or "overfitting") were addressed specifically by grading based on the predominant pattern that represented the majority of the view in each image. Each image was also graded on the basis of the highest histopathological grade observed: that is, if types B and D were observed in a particular image, the final grade would be type D only.

Histology

Biopsy specimens were processed with H&E and alcian blue stains. These were reviewed by an expert gastrointestinal pathologist (PK) who has had extensive experience in gastrointestinal pathology for more than 10 years. The pathologist was blinded to the endoscopic findings. Dysplasia in Barrett's esophagus was classified according to the Vienna classification [16] and confirmed by a second experienced gastrointestinal pathologist. Challenging cases wherein agreement was discordant were reviewed by three or four experienced gastrointestinal pathologists and a final pathological diagnosis representing a consensus was made. Previous studies have shown majority opinion by experienced pathologists to correlate best with outcome [17]. The NBI-Z grading of each image was then compared with the final histopathological diagnosis.

Assessment of interobserver and intraobserver variability

The reproducibility and repeatability of this classification were further assessed by three endoscopists who were unfamiliar with NBI (P. F., K. G., and H. K.; non-NBI-experts) and three endoscopists experienced in the use of NBI (A. S., G. K. A., and K. R.; NBI-experts). All six endoscopists had performed over 1000 upper endoscopies each. The non-NBI-expert endoscopists had not performed any endoscopies using NBI, whereas the NBI-experts had each performed more than 150 NBI procedures and were familiar with the technology. Two hundred and ten digital images of each prebiopsy specimen were selected. For the purpose of this assessment only the predominant pattern of each image which correctly corresponded to the histological diagno-

sis was used. The images were enlarged to fit a 35-mm slide format without distorting the contrast or color balance and were anonymized. Forty of the images (ten of each type) were first shown as a reference guide. The same concerns about visualizing more than one pattern in each image were clearly explained during the initial tutorial phase. This was followed by the evaluation phase, in which the remaining 170 images were graded according to the above classification. To test for intraobserver variability, the exercise was repeated after 1 week with the same images but in a different order.

Statistical analysis

All statistical analysis was performed using the Statistical Package for Social Sciences (SPSS version 14, SPSS Inc., Chicago, Illinois, USA). The positive and negative predictive values for the detection of columnar mucosa without intestinal metaplasia, intestinal metaplasia, low-grade dysplasia (LGD), and high-grade dysplasia (HGD) were calculated. The κ scores for interobserver and intraobserver agreement in the assessment of the various NBI-Z images were also calculated. Agreement was taken as [18]:

- Poor if $\kappa < 0.2$.
- Fair if $0.21 < \kappa < 0.40$.
- Moderate if $0.41 < \kappa < 0.60$.
- Substantial if $0.61 < \kappa < 0.80$.
- Good if $\kappa > 0.80$.

Results

One hundred and nine patients were recruited (77 men; mean age 61.9 years; age range 18 – 86 years), nine of whom were referred for further workup of dysplasia. The mean values (ranges) for the Barrett's length according to the Prague criteria were: circumferential, 3.3 (0 – 13) cm; maximum extent, 4.5 (1 – 14) cm (**Table 1**). Eighty patients had a hiatal hernia associated with the Barrett's segment. All patients were receiving treatment with proton pump inhibitors. The results were assessed on a per-biopsy basis by comparing the grading of each NBI-Z image with the histological diagnosis of the corresponding biopsy. To further demonstrate clinical relevance we felt it was necessary to present the results on a per-patient basis as well, by taking the worst NBI-Z grading in each patient and correlating it with the worst histological diagnosis.

Per-biopsy analysis

A total of 1021 images were obtained and assessed together with their corresponding biopsy specimens. Sixty-four specimens were dysplastic (12 LGD, 52 HGD). On two of these the two pathologists initially failed to achieve agreement; both lesions were classified as LGD on consensus agreement. In 903 areas the NBI-Z grading corresponded to the histological diagnosis, giving it an accuracy of 87.9% (type A pattern: columnar mucosa without intestinal metaplasia, 111/207; types B and C pattern: intestinal metaplasia, 742/750; type D pattern: HGD, 50/52 (**Table 2**). The positive and negative predictive values calculated were thus 100% and 89% respectively for type A, 90% and 96% for types B and C, and 79% and 100% for type D (**Table 3**). There was no difference between the appearance of intestinal metaplasia and LGD on NBI-Z imaging. NBI-Z correctly identified 50 of the 52 areas with HGD.

Table 1 Patient demographics

Total no. of patients	109
Total no. of areas examined/imaged with corresponding biopsies	1021
Sex, no. of patients (male/female)	77/32
Barrett's esophagus length: circumference, mean (range), cm	3.3 (0 – 13)
Barrett's esophagus length: maximal extent, mean (range), cm	4.5 (1 – 14)
Hiatal hernia (mean, range), cm	2.6 (0 – 7)
Histological diagnoses	
Columnar mucosa without intestinal metaplasia	21
Intestinal metaplasia	69
Low-grade dysplasia	5
High-grade dysplasia	14

Per-patient analysis

The worst histological lesion in any given Barrett's segment was used for the per-patient analysis. Of the 109 patients enrolled in the study, dysplasia was detected in the Barrett's segment in 19. Fourteen of these patients exhibited HGD and five LGD (**Table 4**). The positive and negative predictive values for type A pattern were 100% and 97% respectively, for types B and C 88% and 91% respectively, and for type D 81% and 99% respectively (**Table 3**).

Interobserver/intraobserver agreement

210 images were selected, out of which 40 (10 of each pit pattern) were first viewed as a reference guide. The remaining 170 consisted of 12 type A, 71 type B, 52 type C, and 35 type D patterns.

The mean accuracy of prediction of the pit patterns by the non-NBI-experts endoscopists was 83.9% (428/510); in the expert group it was 90.0% (459/510). Overall, the non-expert endoscopists correctly predicted type A pattern in 97% of the images, type B pattern in 83%, type C pattern in 83%, and type D pattern in 84%. The corresponding values for the expert endoscopists

Table 2 Comparison of final histological diagnosis with mucosal patterns on NBI-Z: per-biopsy analysis

NBI-Z pattern	Histological diagnosis				
	CM	IM	Low-grade dysplasia	High-grade dysplasia	Total
A	111	0	0	0	111
B	75	525	9	2	611
C	18	217	1	0	236
D	3	8	2	50	63
Total	207	750	12	52	1021

CM, columnar mucosa without intestinal metaplasia; IM, intestinal metaplasia; NBI-Z, narrow-band imaging with magnification.

NBI-Z pattern (histology)	Per biopsy		Per patient	
	PPV	NPV	PPV	NPV
A (CM)	100 (96 – 100)	89 (87 – 91)	100 (78 – 100)	97 (90–99)
B & C (IM)	90 (87 – 92)	96 (92 – 98)	88 (80 – 94)	91 (75 – 98)
D (HGD)	79 (67 – 88)	100(99 – 100)	81 (54 – 95)	99 (93 – 100)

CM, columnar mucosa without intestinal metaplasia; IM, intestinal metaplasia; NBI-Z, narrow-band imaging with magnification; NPV, negative predictive value; PPV, positive predictive value.

Table 3 Positive and negative predictive values of the per-biopsy and per-patient analysis (% with 95 % CI)

NBI-Z pattern	Histological diagnosis				
	CM	IM	Low-grade dysplasia	High-grade dysplasia	Total
A	18	0	0	0	18
B & C	3	66	5	1	75
D	0	3	0	13	16
Total	21	69	5	14	109

CM, Columnar mucosa without intestinal metaplasia; IM, intestinal metaplasia; NBI-Z, narrow-band imaging with magnification.

Table 4 Comparison of final histological diagnosis with mucosal patterns on NBI-Z: per-patient analysis

Endoscopist	Type A (N = 12)		Type B (N = 71)		Type C (N = 52)		Type D (N = 35)	
	n	%	n	%	n	%	n	%
Non-NBI-expert								
1	12	100	64	90	36	69	30	86
2	12	100	65	92	49	94	24	69
3	11	92	47	66	44	85	34	97
NBI-expert								
1	12	100	59	83	50	96	29	83
2	12	100	69	97	50	96	29	83
3	12	100	56	79	46	88	35	100

Table 5 Accuracy of non-NBI-expert- and NBI-expert-endoscopists in predicting various mucosal patterns

were 100 %, 86 %, 94 %, and 89 % (**Table 5**). Intestinal metaplasia (types B and C) was correctly predicted in 83 % (305/369) of the images by the non-experts and in 89 % (330/369) by the experts, while for HGD (type D) the figures were 84 % (88/105) and 89 % (93/105) by the non-expert and expert groups respectively.

The mean κ value for interobserver agreement in assessing the various patterns in the non-expert group was 0.71 (95 % CI 0.65 – 0.76, $P < 0.001$) and the intraobserver agreement was 0.87 (95 % CI 0.71 – 1.00, $P < 0.001$), whereas the mean values in the expert group were 0.78 (95 % CI 0.73 – 0.83, $P < 0.001$) and 0.91 (95 % CI 0.76 – 1.00, $P < 0.001$) respectively, indicating substantial to good agreement [18].

Discussion

Random quadrantic biopsies have been shown to sample only about 3.5 % of each 2-cm segment of the Barrett's mucosa [19]. This "blind" approach is associated with high sampling errors as dysplastic lesions can arise from flat inconspicuous areas in Barrett's esophagus. Chromoendoscopy with various dyes has been investigated as a tool to increase the yield when targeting these areas [20 – 22], but there are various problems associated with it: sometimes these dyes do not spread uniformly on the surface of the mucosa; they can be messy to prepare; and there have been some concerns regarding toxicity [23]. NBI simulates chromoendoscopy but obviates the use of any dye sprays. With magnification (NBI-Z), visualization of the mucosal surface in Barrett's esophagus is enhanced. This study had two objectives: (i) to validate a simplified NBI-Z classification of mucosal morphology and prediction of histology in Barrett's esophagus in a large cohort of samples (109 patients with more than 1000 corresponding biopsy–image sets), and (ii) to gauge its reproducibility when the NBI-Z images were assessed both by endoscopists experienced in the use of NBI and by those new to NBI.

On the basis of the 1021 areas visualized, NBI-Z allowed correct prediction of 99 % of the areas with intestinal metaplasia and 96 % of the areas demonstrating HGD. These findings were not different from those reported in previous studies which attempted to characterize the mucosal morphology in Barrett's esophagus. Sharma et al. [11] reported the morphology in Barrett's esophagus on the basis of the mucosal and vascular patterns separately. Using the mucosal patterns as the basis for assessment, the PPV in the prediction of intestinal metaplasia was 95 % and that for HGD was 95.3 %. Using the vascular patterns, the PPV for HGD was 94.7 %.

In our study, 2 out of 52 areas which exhibited HGD were missed when the NBI-Z mode was used to characterize the area. These were reported as exhibiting a type B pattern with regular villous/ridge pattern and vasculature. This equated to missing a significant pathology in 1 of the 109 patients (both biopsies were from the same patient), and this must be considered as a major drawback of this study. However, further analysis of the biopsy specimens revealed that both the samples concerned harbored the dysplasia in the deeper layers, which could very well have been beyond the penetration of the NBI-Z, and this could have accounted for the discrepancy. One of the other drawbacks is that we were unable to clearly differentiate intestinal meta-

plasia from LGD on NBI-Z views in the way as was depicted by previous studies. Out of the 12 biopsies reported as showing LGD, 9 (75 %) exhibited type B morphology, 1 type C, and 2 type D. On reassessing these images, we were unable to identify any salient features which could clearly distinguish any typical morphologic features seen on NBI-Z in LGD compared to the other histological grades. One plausible explanation is that the mucosal or vascular changes associated with LGD may not be significantly different from nondysplastic areas at the current magnification level. It must, however, be stressed that the diagnosis of LGD itself is almost always contentious, with high interobserver variability seen even among expert pathologists [17]. It would be interesting to study the morphologic patterns in greater detail in a larger group of patients specifically with LGD. Although NBI-Z exhibited high positive and negative predictive values for columnar mucosa without intestinal metaplasia, the sensitivity was disappointing at 54 % (95 % CI 0.47 – 0.61), albeit the specificity was 100 % (95 % CI 0.99 – 1.00). This finding could, however, be interpreted as of less significance given the benign nature of columnar mucosa without intestinal metaplasia.

In the selection of images for the interobserver and intraobserver assessment, it could be deduced that only high-quality images were used (210/1021). We were aware of this limitation, but given the enormous task of grading more than 1000 images twice, we opted to limit the assessment to only 210 images. Moreover, it is important to obtain the best images when performing such a study since the assessors would not have the advantage of real-time viewing. Nevertheless, selection bias must also be considered as one of the drawbacks of this study. Grading 210 images at once too can be interpreted as "overideal" as in practice these numbers would certainly be achieved over a much longer time frame. Hence, the fact that the previous images were fresh in the minds of the assessors must also be taken into consideration. It must also be stressed that the observer agreement is valid only in terms of the interpretation of the images, not the actual process of obtaining the images.

The present study differed in some ways from previously published descriptive studies. Sharma and colleagues [11] did not characterize the NBI-Z views of the Barrett's esophagus segment exhibiting absent pit patterns as was depicted by the type C phenotype in our study. This morphologic pattern was encountered in almost one in five of our patients (236/1021 biopsies) and was also reported by the Amsterdam group [12]. Kara et al. [12] characterized the different patterns visualized in the Barrett's segment by adding an additional component to the description. In addition to assessing the pit pattern and vasculature, the group found a third element in the characterization of Barrett's mucosa: abnormal blood vessels, which were found to be increasingly associated with the progression of dysplasia. However, it was unclear how this element was different from irregular vasculature and whether its addition was practically feasible. We found the proposed multistep "hierarchical classification" complicated, and therefore embarked on a different approach to the classification of the various different morphologic patterns visualized in Barrett's esophagus. After reviewing images from our preliminary observational study, we devised a simplified formula which we found to be practical and reproducible. This was clearly shown by the high accuracy and the "substantial to good" interobserver and intraobserver agreement exhibited by both the NBI-expert and the non-NBI-expert endoscopists in our study.

In conclusion, this study has not only validated a simplified classification of the various morphologic patterns visualized in Barrett's esophagus and corresponding histology, with high predictive values, but also confirmed its reproducibility and repeatability when used by both endoscopists experienced in the use of NBI and those unfamiliar with it. A randomized controlled study comparing this novel technique using this classification with conventional random four-quadrant biopsies in the detection of dysplasia would ideally be the next step forward. It is hoped that the abandonment of separate evaluations for pit morphology, abnormal blood vessels, and microvascular patterns, as in previous classifications, and instead combining them in a simplified manner may lead to improved applicability of NBI with magnification in Barrett's esophagus in clinical practice.

Competing interests: Dr. Ragunath has received educational grants, speaker honorarium and research support in the form of prototype endoscopy equipment from Olympus-Keymed, UK.

References

1 *Devesa SS, Blot WJ, Fraumeni JF Jr.* Changing patterns in the incidence of esophageal and gastric carcinoma in the United States. Cancer 1998; 83: 2049 – 2053
2 *Jankowski J, Provenzale D, Moayyedi P.* Oesophageal adenocarcinoma arising from Barrett's metaplasia has regional variations in the West. Gastroenterology 2002; 122: 588 – 590
3 *Enzinger PC, Mayer RJ.* Esophageal cancer. N Engl J Med 2003; 349: 2241 – 2252
4 *Streitz JM Jr, Andrews CW, Ellis FH.* Endoscopic surveillance of Barrett's esophagus. Does it help? J Thoracic Cardiovasc Surg 1993; 105: 383 – 387
5 Guidelines for the diagnosis and management of Barrett's columnar-lined oesophagus. A report of the Working Party of the British Society of Gastroenterology August 2005. Available at http://www.bsg.org.uk/pdf_word_docs/Barretts_Oes.pdf. Accessed 20 March 2008
6 *Sampliner RE.* Updated guidelines for the diagnosis, surveillance and therapy of Barrett's oesophagus. Am J Gastroenterol 2002; 97: 1888 – 1895
7 *Cameron A, Carpenter HA.* Barrett's esophagus, high grade dysplasia, and early adenocarcinoma: a pathological study. Am J Gastroenterol 1997; 92: 586 – 591
8 *Van Dam J.* Novel methods of enhanced endoscopic imaging. Gut 2003; 52: 12 – 16
9 *Hamamoto Y, Endo T, Nosho K et al.* Usefulness of narrow band imaging endoscopy for diagnosis of Barrett's oesophagus. J Gastroenterol 2004; 39: 14 – 20
10 *Anagnostopoulos GK, Yao K, Kaye P et al.* Novel endoscopic observation in Barrett's oesophagus using high resolution magnification endoscopy and narrow band imaging. Aliment Pharmacol Ther 2007; 26: 501 – 507
11 *Sharma P, Bansal A, Mathur S et al.* The utility of a novel narrow band imaging endoscopy system in patients with Barrett's esophagus. Gastrointest Endosc 2006; 64: 167 – 175
12 *Kara MA, Ennahachi M, Fockens P et al.* Detection and classification of the mucosal and vascular patterns (mucosal morphology) in Barrett's esophagus by using narrow band imaging. Gastrointest Endosc 2006; 64: 155 – 166
13 *Playford RJ.* New British Society of Gastroenterology (BSG) guidelines for the diagnosis and management of Barrett's oesophagus. Gut 2006; 55: 442 – 443
14 *Gono K, Obi T, Yamaguchi M et al.* Appearance of enhanced tissue features in narrow-band endoscopic imaging. J Biomed Opt 2004; 9: 568 – 577
15 *Sharma P, Dent J, Armstrong D et al.* The development and validation of an endoscopic grading system for Barrett's esophagus: the Prague C & M criteria. Gastroenterology 2006; 131: 1392 – 1399
16 *Dixon MF.* Gastrointestinal epithelial neoplasia: Vienna revisited. Gut 2002; 51: 130 – 131
17 *Skacel M, Petras RE, Granlich TL et al.* The diagnosis of low grade dysplasia in Barrett's esophagus and its implication for disease progression. Am J Gastroenterol 2000; 95: 3383 – 3387

18 *Landis JR, Koch GG.* The measurement of observer agreement for categorical data. Biometrics 1977; 33: 159 – 174
19 *Boyce HW.* Barrett's esophagus: endoscopic findings and what to biopsy. J Clin Gastroenterol 2003; 36 (Suppl): S6 – S18
20 *Canto MI, Setrakian S, Willis J et al.* Methylene blue-directed biopsies improve detection of metaplasia and dysplasia in Barrett's oesophagus. Gastrointest Endosc 2000; 51: 560 – 568
21 *Sharma P, Weston AP, Topalovski M et al.* Magnification chromoendoscopy for detection of intestinal metaplasia and dysplasia in Barrett's oesophagus. Gut 2003; 52: 24 – 27
22 *Fortun PJ, Anagnostopoulos GK, Kaye P et al.* Acetic acid-enhanced magnification endoscopy in the diagnosis of specialised intestinal metaplasia, dysplasia and early cancer in Barrett's oesophagus. Aliment Pharmacol Ther 2006; 23: 735 – 742
23 *Olliver JR, Wild CP, Sahay P et al.* Chromoendoscopy with methylene blue and associated DNA damage in Barrett's esophagus. Lancet 2003; 362: 373 – 374